Tuning polymer melt fragility with antiplasticizer additives

Robert A. Riggleman
Department of Chemical and Biological Engineering, University of Wisconsin-Madison, Madison, Wisconsin 53706

Jack F. Douglas
Polymers Division, National Institute of Standards and Technology, Gaithersburg, Maryland 20899

Juan J. de Pablo
Department of Chemical and Biological Engineering, University of Wisconsin-Madison, Madison, Wisconsin 53706

(Received 23 January 2007; accepted 27 April 2007; published online 19 June 2007)

A polymer-diluent model exhibiting antiplasticization has been developed and characterized by molecular dynamics simulations. Antiplasticizer molecules are shown to *decrease* the glass transition temperature T_g but to *increase* the elastic moduli of the polymeric material in the low-temperature glass state. Moreover, the addition of antiplasticizing particles renders the polymer melt a stronger glass-forming material as determined by changes in the characteristic temperatures of glass formation, the fragility parameter D from fits to the Vogel-Folcher-Tamman-Hesse equation, and through the observation of the temperature dependence of the size of cooperatively rearranging regions (strings) in each system. The length of the strings exhibits a weaker temperature dependence in the antiplasticized glass-forming system than in the more fragile pure polymer, consistent with the Adam-Gibbs model of glass formation. Unexpectedly, the strings become increasingly concentrated in the antiplasticizer particles upon cooling. Finally, we discuss several structural indicators of cooperative dynamics, and find that the dynamic propensity (local Debye-Waller factor $\langle u^2 \rangle_p$) does seem to provide a strong correlation with local molecular displacements at long times. The authors also consider maps of the propensity, and find that the antiplasticized system exhibits larger fluctuations over smaller length scales compared to the pure polymer. © *2007 American Institute of Physics*. [DOI: 10.1063/1.2742382]

I. INTRODUCTION

The addition of small amounts of solvent to a polymeric system normally leads to a depression of the glass transition temperature T_g and a softening of polymeric materials. This "plasticization" phenomenon is widely exploited in applications[1,2] and has been the subject of numerous experimental and theoretical studies. Considerably less effort, however, has been devoted to the study of "antiplasticizers"—a special class of molecules with the ability to lower the glass transition, while *simultaneously increasing* the elastic moduli (or stiffness) of polymeric materials in the glassy state. Examples of antiplasticizer/polymer pairs include tricresyl phosphate in polysulfonate[3] and dibutylphthalate in polycarbonate.[4]

A variety of explanations of antiplasticization have been suggested.[5–10] One prevalent idea is that the antiplasticizer interacts strongly with the polymer chains and acts like a cross-linking agent.[5] A strong interaction between the antiplasticizer and the polymer has also been proposed to give rise to an adsorbed layer of solvent about the polymer that slows down fast molecular motions.[10] Others have suggested that antiplasticizer molecules fill the "holes" that arise in the polymer from free volume fluctuations, and a number of models have been introduced based on this simple physical viewpoint. Ngai *et al.* and Rizes *et al.*,[7,8] however, have presented evidence that challenges the popular free-volume concept of the origin of antiplasticization, and so the interpretation of this phenomenon remains unresolved, even from a qualitative standpoint. We must also recognize that this phenomenon may have more than a single cause and the mechanisms mentioned above may each be partially correct.

Glass-forming materials are often characterized in terms of their so-called "fragility," which measures the rate at which various relaxation processes change with temperature as T_g is approached from above. For a fragile glass former, for example, the viscosity increases dramatically when the temperature approaches T_g (by as many as ten orders of magnitude for a 20 degree change in temperature). In contrast, the viscosity of a strong glass former normally changes more gradually with temperature. Recent theoretical arguments[11] suggest that the fragility variations in polymeric liquids derive from differences in the packing efficiency of these complex-shaped macromolecules as a function of the monomer structure, interactions, and thermodynamic parameters such as the pressure. Polymeric fluids such as polystyrene and polycarbonate, with stiff, bulky side groups or backbones, are found to exhibit a large degree of packing frustration and are thus "fragile" glass formers.[11] This simple physical picture of fragility changes in polymer fluids suggests that it should be possible to *modulate* the fragility through the addition of miscible nanoparticles and certain solvents (such as antiplasticizers) having dimensions smaller than the

statistical segment size. In particular, we would expect such particles to become localized into regions of space where the packing frustration is large. A reduction of T_g would be expected to occur, and in addition such particles would be expected to increase the density and the stiffness of the mixture in the glassy state. Our hypothesis is that such additives should lead to a reduction of the fragility (measured in this work as the strength of the temperature dependence of structural relaxation) and a reduction of the scale of cooperative segmental motion.[11,12]

To the best of our knowledge, antiplasticization has not been considered before in terms of an explicit molecular computational model, and it is the goal of this work to develop and characterize such a model and study the effects of antiplasticization on the fragility of a model polymer. In this work, a small-molecule solvent is added to a coarse-grain polymer melt. The polymer model is chosen to be a fragile glass former that has been characterized extensively.[13] We begin by presenting the model below, then obtaining several characteristic temperatures, estimates of the fragility (the strength of the temperature dependence of the structural relaxations), and the elastic moduli of both the pure polymer and antiplasticized systems. We find that the small molecules antiplasticize the mixture by increasing the density below $T_{g,\mathrm{pure}}$, decreasing T_g, and enhancing the shear modulus in the glassy state. We also find that the antiplasticizer particles make the system a stronger glass former, as characterized by the strength of the temperature dependence of the relaxation times. Additionally, our results are consistent with the simple picture of glass formation proposed by recent theories,[11,14] which suggests that differences in fragility are due to differences in packing frustration, where better packing leads to a stronger glass formation. This is what we observe, where the more dense, antiplasticized melt is a stronger glass former than the fragile, pure polymer melt.

Additionally, we investigate how antiplasticization modifies the relaxation of the polymer by characterizing the tendency of the system to relax via the string like collective motion, which has been previously identified with the cooperatively rearranging regions of Adam and Gibbs.[12,15] We find that as the temperature is lowered into the supercooled regime for the antiplasticized mixture the rearranging regions consist of a larger fraction of the antiplasticizing particles, while the number of particles involved in the rearrangement changes by a minimal amount. In the pure polymer system, the rearranging regions become larger as temperature is decreased. Finally, we investigate several structural indicators of fast dynamics in the pure polymer system. We find that both the local deviation from tetrahedral packing and the short-time mean-squared displacement ("propensity" or *local* Debye-Waller factor $\langle u^2 \rangle_p$) are both sensitive to long-time mobility. Moreover, the spatial fluctuations of the propensity are much more intense in the antiplasticized system, even though these systems are more dense in the glassy state.

II. METHODS

Our molecular dynamics (MD) simulations employ a coarse-grained model of a polymer melt with and without an antiplasticizer additive. The pure polymer melt has been extensively characterized in previous works,[13,16–18] and here we merely provide its main elements. Each polymer molecule consists of 32 Lennard-Jones spherical interaction sites connected by harmonic springs with a force constant of $2000\epsilon/\sigma^2$. We modify the standard Lennard-Jones potential slightly to the following form:

$$U(r) = v(r) - v(r_c) - \left[\frac{dv(r)}{dr}\right](r - r_c), \tag{1}$$

for $r \leqslant r_{\mathrm{cut}}$ and zero otherwise, where

$$v(r) = 4\epsilon\left[\left(\frac{\sigma}{r}\right)^{12} + \left(\frac{\sigma}{r}\right)^{6}\right]. \tag{2}$$

This ensures that both the potential energy and its first derivative go smoothly to zero at r_{cut}. The Lennard-Jones parameters for polymer monomers (A) are taken to be unity; for the antiplasticizer (B), we use $\epsilon_B = \epsilon_A = 1.0$ and $\sigma_B = 0.5$. Equal values of epsilon helps to promote entropic mixing in the system, while the smaller value of σ_B promotes more efficient packing upon addition of the antiplasticizer particles. Lorentz-Berthelot combining rules are used for cross interactions. The mass of a polymer monomer is unity and that of an antiplasticizer particle is 0.125, consistent with the relative volume of each species. All units in this paper are in Lennard-Jones units of the polymer monomer (i.e., $T/T^* = k_B/\epsilon_A$, $P/P^* = \sigma_A^3/\epsilon_A$, $t/t^* = \sqrt{\sigma_A^2 m/\epsilon_A}$, where the * implies real units, and R is the gas constant). Our time step δt was taken to be $\delta t = 0.001$. If ϵ is taken to be approximately $300k_B$, and σ_A approximately as 2 nm [a typical statistical segment size for poly(methyl methacrylate)], then the unit time is roughly 20 ps. Since equilibrium MD simulations are necessarily restricted to temperatures considerably larger than T_g (e.g., $T/T_g \geqslant 1.2$), we pursue multiple accessible measures of fragility that apply to the high-temperature regime of glass formation, as well as relaxation-time extrapolations to the low-temperature regime of glass formation.

Systems were equilibrated at $T^* = 1.0$, and independent configurations were generated at this temperature by performing MD simulations until the end-to-end correlation function had decayed for our systems. MD simulations were carried out at zero pressure for 10^7 time steps, after which the temperature was lowered in increments of 0.01 per 100 000 time steps to the desired temperature. This was followed by performing *N-P-T* simulations for 10^6 time steps in order to obtain the average density at each temperature. Finally, the production runs were performed in the *N-V-T* ensemble at the obtained average density. This protocol was employed to enable a direct comparison with experiments, which are performed at constant pressure rather than constant volume. Our simulation boxes contained 50 polymer chains plus 674 antiplasticizer particles (5% by mass or 29.6% by moles). Such a composition roughly corresponds to the value for which antiplastification is more pronounced in experiments, and in our model it corresponds to noticeable and unambiguous changes of the relaxation of the polymer (without diluting it too much).

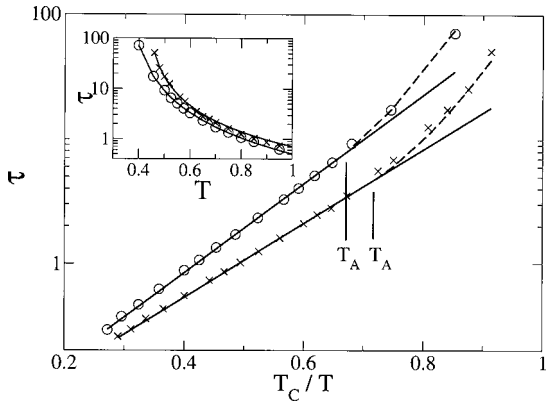

FIG. 1. Relaxation times τ obtained from the bond autocorrelation function for the pure polymer (×) and the antiplasticizer (○). The solid lines are fits of high-temperature results using Eq. (4) the Arrhenius equation. Approximate values of T_A are indicated in the figure; the dashed lines indicate a fit to Eq. (6) $E_a(T)$. The inset shows fits of τ using Eq. (3).

III. DYNAMIC PROPERTIES AND FRAGILITY CHARACTERIZATION

The structural relaxation time τ is one of the basic properties that characterize glass formation; our estimates of fragility largely revolve around the calculation of τ as a function of temperature. A variety of structural relaxation processes can be chosen to examine the rate of structural relaxation. The bond autocorrelation function provides a particularly useful and simple means for defining a relaxation time in our model polymers, and has been shown in previous works to give results equivalent to those obtained from analyzing the dynamic structure factor.[19] The characteristic relaxation time τ was taken as the time where the bond autocorrelation function decayed to $1/e \approx 0.368$. The values of τ for each system are shown in Fig. 1. The uncertainty associated with τ was calculated by creating two additional independent configurations for each system at high temperature and repeating the cooling procedure described above. We then calculated the bond autocorrelation function to determine τ for the new configurations. The largest run-to-run variations were found at our lowest temperature, where the variations were approximately 10%. At each other temperature, the uncertainty was less than 4%. Nevertheless, when we propagate the uncertainties to the characteristic temperatures described below, we conservatively use a 10% uncertainty on all values of τ. The uncertainties were determined on the characteristic temperatures using a first-order sensitivity analysis. The inset in Fig. 1 shows that the additive leads to a modest reduction of τ over the temperature range considered in this work. The differences in the relaxation times between the two systems become more apparent as the temperature is decreased. At the lowest temperature investigated for the pure polymer, the difference is approximately a factor of 3. The differences between data for the pure polymer and the mixture become even more apparent if we consider the Arrhenius-plot representation shown in the main part of Fig. 1. In this plot, we introduce a reduced temperature T/T_c by fitting τ to an expression of the following form:

$$\tau = A(T - T_c)^{-\gamma}. \tag{3}$$

Equation (3) is inspired by mode-coupling theory and the empirically fitted temperature T_c is often designated the "mode-coupling temperature." The entropy theory of Dudowicz *et al.*[11] indicates that T_c has a well-defined thermodynamic significance as a crossover temperature which approximately delineates the boundary between the high- and low-temperature regimes of glass formation. We thus consider this characteristic temperature to have a similar significance in this work. We find $T_c = 0.42$ and 0.34 for the pure polymer and the antiplasticizer system, respectively, and $\gamma = 1.59$ and 2.01. The standard relative uncertainties associated with T_c were less than 2%. Previous numerical studies of glass-forming liquids have shown that T_c approximately delineates the high- and low-temperature regimes of glass formation; we view it in this work as a well-defined characteristic temperature of glass formation.

Another characteristic temperature of glass formation is indicated in Fig. 1. We denote this temperature as T_A, and it corresponds to the point at which τ ceases to exhibit an Arrhenius behavior.[20] For the pure polymer and the mixture T_A is found to be 0.59 and 0.51, respectively. We estimate the uncertainty on T_A to be less than 0.01. Above T_A, we can fit our relaxation times to the Arrhenius equation,

$$\tau = \tau_A \exp[-E_a/k_B T]. \tag{4}$$

Here, τ_A is the high-temperature relaxation time and E_a is the activation energy. We find E_a to be 2.87 and 2.80 and that τ_A is 0.035 and 0.032 for the pure and antiplasticized systems, respectively. Experimental values of τ_A are typically on the order of 10^{-13} s.[21]

Two other common characteristic temperatures are T_g, which operationally marks the point where the fluid tends to drop out of equilibrium in laboratory experiments, and T_0, which is the so-called Vogel temperature, and signals the "end" of the glass transition range where τ extrapolates to infinity.[22] The estimation of these temperature's from molecular dynamics simulations is necessarily much more uncertain than that of T_c or T_A due to the large extrapolations required. Keeping this uncertainty in mind, we determine T_g and T_0 by fitting our relaxation time results to the so-called Vogel-Fulcher-Tammann-Hesse equation,[22]

$$\tau = \tau_0 \exp\left[D\frac{T_0}{T - T_0}\right], \tag{5}$$

where τ_0 is a prefactor with units of time. We note that τ_0 differs from τ_A, the prefactor of the Arrhenius equation [Eq. (4)]. Strictly speaking, within the framework of the entropy theory of glass formation[11] Eq. (5) is valid in the temperature range between T_c and T_g, while equilibrium simulations are generally restricted to temperatures above T_c. Reasonable estimates of τ based on Eq. (5) in both simulations and experiments can be obtained for a temperature range slightly above T_c. Accordingly, we only fit our data to our six lowest temperature data points, as shown in the inset to Fig. 1. We perform this fitting in order to obtain an estimate for T_g and T_0; we note that fitting above T_c has been considered by previous authors[23–25] and our results discussed below are

consistent with previous findings. Once we have estimated the temperature dependence of τ in the low-temperature regime as best we can from molecular dynamics simulations, T_g is prescribed by the rather standard physical condition that $\tau(T_g)=O(100\ \mathrm{s})$; T_0 is determined by fitting the relaxation time data of Fig. 1 to Eq. (5). We emphasize the appreciable uncertainty due to the large extrapolation, and the uncertainties associated with T_0 and T_g are found to be approximately 8%. Fitting our results to Eq. (5) for the lowest temperatures investigated for each system gives $T_0=0.34$ and 0.23 for the pure and the antiplasticized mixture, respectively. As discussed below, an important test of the validity of this approach is to compare the results obtained through fits to Eq. (5) to results for other systems.

The parameter D, which is sometimes viewed as a measure of fragility "strength," is correspondingly determined from our fit to Eq. (5) to be 1.54 and 4.24 in the pure polymer and the mixture, respectively. In our dimensionless units τ_0 is found to be of order unity ($\tau_0=0.98$ and 0.66 for the pure polymer and the mixture, respectively). In this work the temperature for glass formation is therefore assigned to the condition $\tau/\tau_0 \sim 10^{15}$ in Eq. (5) resulting in $T_g=0.36$ and 0.25 for the pure polymer and the mixture, respectively.

Regardless of the physical interpretation that one may wish to adopt, the fragility of a glass former is first and foremost a measure of deviation from the Arrhenius temperature dependence of relaxation times that is commonly observed in most fluids at high temperatures. As can be seen in Fig. 1, the deviation from the Arrhenius behavior is not limited to temperatures in the immediate vicinity of T_g. However, entropy-based theories of glass formation predict that, below T_A, the apparent activation energy $E_a(T\to\infty)$ should follow a universal quadratic temperature dependence of the following form:

$$\frac{E_a(T)}{E_a(T\to\infty)} \sim \left[1 + C_0\left(\frac{T-T_A}{T_A}\right)^2\right], \tag{6}$$

where the coefficient C_0 is a direct measure of fragility.[11] For the pure polymer and the mixture considered in this work, we find $C_0=2.93$ and 2.26, respectively, and $E_a(T\to\infty)$ (units of kT_c) equals 6.3 and 7.3. The reduction of C_0 upon addition of small particles provides unambiguous evidence that the temperature dependence of relaxation is weakened by the additive, i.e., the fragility is reduced.

Further evidence that the fragility is reduced by the addition of particles can be obtained by examining the ratios of various characteristic temperatures. These ratios, which we report in Table I, provide some of the strongest, model-independent indicators of fragility; large ratios of the characteristic temperatures are indicative of relatively strong glass-forming liquids. Also included in the table is the so-called "fragility index," $K_s=1/D$ obtained by fitting results in Fig. 1. The ratios of characteristic temperatures of glass formation are all markedly larger for the polymer-particle mixture, confirming that it is stronger than the pure polymer. It is also reassuring that the actual values of these ratios are in agreement with those obtained from theoretical calculations based on entropy-based models of the glass transition[11] (such estimates have been included in Table I for completeness and experimental values for fragile and strong polymers[11]). This is true even for the characteristic temperatures obtained from Eq. (5), which require substantial extrapolation to lower temperatures and which are necessarily more uncertain.

TABLE I. Fragility parameter $K_s=1/D$ and ratios of the characteristic temperatures for the pure polymer (PP) and antiplasticized polymer (AP) system. Also included are values of the same ratios from Ref. 11 for the fragile (FS) and strong (FF) glass-forming polymers with a molecular mass $M=101$. The run-to-run variation of the numerical estimates shown here and in the text of the paper is less than 2%.

Parameters	PP	FS	AP	FF
K_s	0.44	0.31	0.17	0.18
C_0	2.93	6.53	2.26	2.79
T_c/T_g	1.25	1.20	1.40	1.39
T_c/T_0	1.32	1.32	1.52	1.65
T_A/T_c	1.33	1.41	1.46	1.56
T_A/T_g	1.71	1.70	2.04	2.16
T_A/T_0	1.76	1.86	2.22	2.56

Up to this point, our studies of the behaviors of τ and its temperature dependence establishes that our small-molecule additives decrease the value of each of the characteristic temperatures of glass formation. Also, by every measure examined, the additives make the melt a stronger glass former, and the physical picture that is emerging is consistent with a new entropy-based theory of glass formation.[11] The reduction in the characteristic temperatures is only one behavior required for this system to be a true antiplasticizer, and we now proceed to demonstrate that our small-molecule solvents also increase the density and moduli of the system at low temperatures.

Five configurations generated at $T^*=1.5T_g^*$ were cooled to the temperatures shown in Fig. 2. After cooling, they were further equilibrated at the temperature of interest for one million time steps in a N-P-T ensemble. Finally, the shear modulus G' was calculated form the response to a sinusoidal strain of the system using Lees-Edwards boundary conditions in conjunction with the SLLOD algorithm.[26] Our system was oscillated with a frequency of $\omega=0.03$ and a maxi-

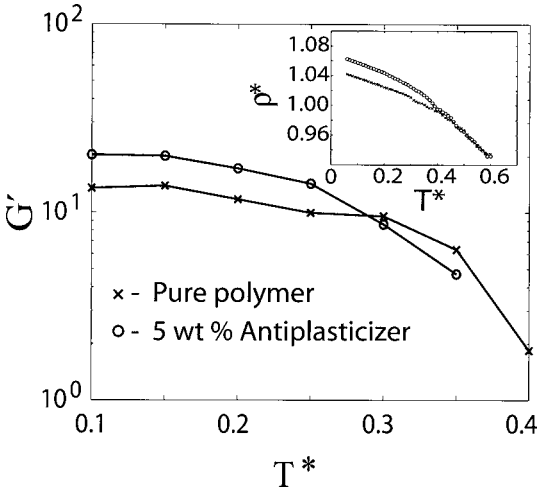

FIG. 2. Shear modulus for the pure polymer and the polymer/antiplasticizer mixture. The inset shows the density of each system as a function of temperature.

mum strain of 0.01. This frequency is approximately two orders of magnitude smaller than that corresponding to the maximum of the Boson peak for these systems, where $\omega_{\text{boson}} \approx 2.5$. To ensure that our strains were still within the linear regime, we confirmed the simulated moduli for select systems by using a maximum strain of 0.005. Figure 2 shows G' as a function of temperature for both the pure polymer and the antiplasticized polymer. The shear modulus of the antiplasticized system is significantly higher than that of the pure polymer, and its modulus begins to decrease at a lower temperature. Additionally, from the inset in Fig. 2, it is observed that below T_g of the pure polymer melt the antiplasticized system shows an enhanced density. Along with the smaller value of T_g indicated above, these observations confirm that the small particles added to the polymer act indeed as an antiplasticizer.

IV. COOPERATIVE DYNAMICS

The structural relaxation of glass-forming liquids is widely believed to occur in the form of collective rearrangements.[11,12,27,28] These rearrangements lead to so-called dynamical heterogeneities, whose existence has been inferred from a variety of experimental measurements. It is therefore of interest to examine how the antiplasticizer particles affect the structural relaxation mechanisms in the glassy state. Simulations of simple glass formers above T_g indicate that the structural relaxation of glass-forming liquids occurs in the form of stringlike collective rearrangements.[15,29,30] A string-cluster analysis was performed to examine the nature of the structural relaxations that occur over a time window Δt^*. We employ a definition of a string motion similar to that used in the literature,[15,29,30] where two particles i and j are part of the same string if Eq. (7) is satisfied,

$$\min[|\mathbf{r}_i(0) - \mathbf{r}_j(t^*)|, |\mathbf{r}_j(0) - \mathbf{r}_i(t^*)|] < \delta. \tag{7}$$

Here, $\mathbf{r}_i(0)$ and $\mathbf{r}_i(t^*)$ are the positions of particle i at an initial time and after a time Δt^*, respectively; δ was taken to be $0.6\sigma_{ij}$. The inclusion of σ_{ij} in δ adjusts the algorithm for the size discrepancy between the antiplasticizer particles and the polymer monomers and has a very small effect on the results. Physically, this algorithm searches for those particles that replace the position of a neighboring particle as the system relaxes. The value of Δt^* is determined from a maximum in the non-Gaussian calculated for the polymer monomers. The most mobile particles were analyzed for a stringlike cooperativity, where the mobile particles were defined as those which had moved farther than the Gaussian prediction over the time Δt^*. This fraction turned out to be 6% for the pure system and 23% for the antiplasticized system. The percentage is so large for the antiplasticized system because there was a substantial number of highly mobile small particles; however, the smaller string lengths discussed below justify the examination of such a large number. See Ref. 28 for further details on our definitions of the strings in the antiplasticized system.

Figure 3 shows the probability of finding strings of different lengths L_s for the pure polymer and antiplasticized mixture at different temperatures for each system; note that each temperature corresponds to approximately the same reduced temperature T/T_c. We find striking differences in the behavior of the two systems. At shorter string lengths ($2 \leqslant L_s \leqslant 9$ at $T = 1.15T_c$), the pure polymer has a higher probability of moving via the stringlike mechanism. However, the antiplasticized system has the ability to form strings that are much more extended than those observed in the pure polymer system, though these extended strings do not occur with a high probability. Indeed, the average string length (discussed below) is smaller for the antiplasticized system when the comparison is made at the same reduced temperature. One expects that more fragile glass formers should on the average require larger numbers of particles to relax than strong glass formers,[12,14,27] and this is exactly the effect we observe. This quantity should also have a weaker temperature dependence, and again this is the trend we find. It is interesting that, although the antiplasticizing material is a stronger glass former, it still has the ability to form large strings. However, on the average, the strings are shorter under similar reduced temperature conditions (see Fig. 4). Our observations here, where we directly compare a strong and

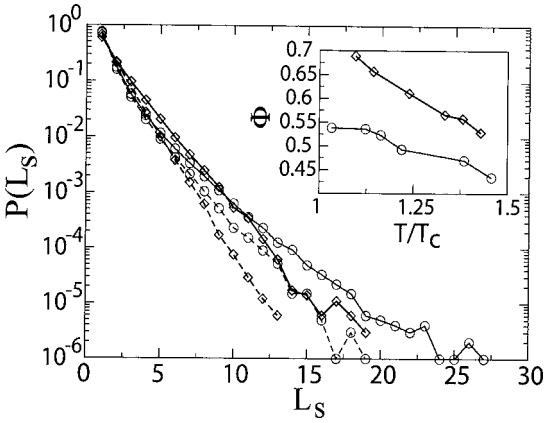

FIG. 3. Probability of finding a string of length L_s for the pure polymer ($\diamond$) and the antiplasticized system ($\bigcirc$). The solid and dashed lines are for $T/T_c \approx 1.15$ and 1.40, respectively. The inset shows the degree of cooperativity of the strings for each system as a function of temperature.

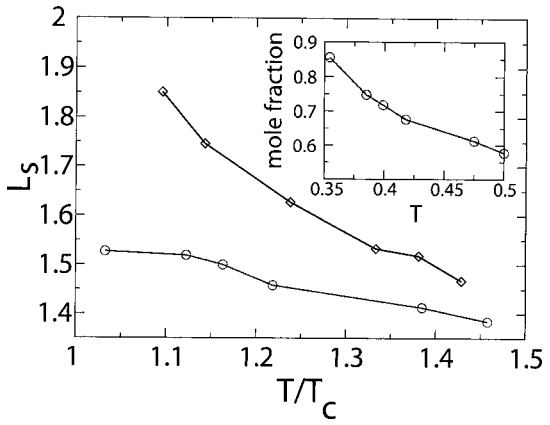

FIG. 4. Mean string length at different temperatures for the pure polymer ($\diamond$) and the antiplasticized system ($\bigcirc$). The inset shows the average composition (mole fraction) of the strings with a length greater than one for the antiplasticized system. The bulk value of ϕ is 0.296.

fragile glass former, could partially explain the results of Ref. 31, where highly extended strings were found in the archetype strong glass former silica. We observe a similar trend where our strong glassformer is able to form highly extended strings; however, it is the average string length and its temperature dependence which determine the relative fragilities.[32] It is also noteworthy that the string length distribution does not appear to be exponential in our antiplasticized system, as they are in our pure polymer and as they have been found in previous works.[15,29,33] The more appreciable deviations from exponential scaling observed in our antiplasticizer results are likely due to our inclusion of the antiplasticizer particles in the definitions of the strings, whereas previous works studying mixtures have only included the major component[15] or considered the two components separately.[33]

A "degree of cooperativity" for the glass-forming liquid Φ can be defined by the fraction of mobile particles in the "cooperative" state of strings, where $L_s \geqslant 2$; Φ is shown in the inset of Fig. 3 for the pure and antiplasticized systems at each temperature. It can be seen that the relative number of particles involved in cooperative strings is reduced through antiplasticization at a common reduced temperature, and that Φ has a weaker temperature dependence than the same quantity for the pure polymer.

A further evidence that the polymer is a more fragile glass former is seen in the temperature dependence of the average string length (L_s) for each system shown in Fig. 4.[32] The average length for the antiplasticized system is nearly constant, while for the pure polymer there is a more appreciable temperature dependence.[32] Also shown in the inset of Fig. 4 is the average composition (mole fraction ϕ) of the strings in the antiplasticizer mixture at each temperature. The bulk value of ϕ is 0.296. Interestingly, although the average length does not have a strong temperature dependence, ϕ changes appreciably and consists of a large fraction of antiplasticizer particles at the lowest temperatures considered here.

V. STRUCTURAL INDICATIONS OF MOBILITY AND LOCAL ELASTIC CONSTANTS

While the development of collective particle motion is one of the most dramatic phenomena observed in supercooled liquids, this collective motion by itself is not responsible for the increase of the structural relaxation time of glass-forming liquids. The collective motion actually serves to reduce the viscosity and it is the growth of the population of relatively immobile particles that is the true origin of the viscosity divergence upon cooling. Questions then arise of how does one achieve a more balanced picture of the supercooled liquid that gives mobile particles appropriate emphasis and how can one investigate a given configuration and determine which particles will have a high or low mobility. Numerous quantities have been investigated in previous works to study this very problem.[16,34,35] For instance, it was recently found that a particle's residence time in a local energy minimum was influenced by the quality of the packing surrounding the particle.[16] Previous experimental works have shown a connection between the system's short-time dynamics and the dynamics over longer time scales,[36,37] and recently Widmer-Cooper and Harrowell[34] have confirmed computationally that the short-time dynamics are a good indicator of the long-time dynamics in glassy systems on a local level.

We have investigated similar properties in our pure polymer system to test whether cooperative dynamics show similar indicators in the structure and the short-time dynamics in both antiplasticized and pure polymer melts. Additionally, our previous works have shown that some insight into the heterogeneities of glassy materials in the low-temperature regime can be obtained by investigating the local elastic constants. These were determined by analyzing the stress fluctuations in a local volume.[38,39] This allows for the construction of a "stiffness map" of the system which shows that the glass is actually a heterogeneous structure exhibiting domains of relatively high stiffness interpenetrated (mechanically unstable) by regions of *negative* stiffness (see Fig. 3 of Ref. 18). Unfortunately, this method of computing elastic constants requires that the material be elastic, a condition that only applies for glasses at low temperatures. At higher temperatures, above T_g, where the viscous response of the system becomes prevalent, these methods do not apply in any simple way.

Recent work has suggested that the Debye-Waller factor, the mean-square particle displacements $\langle u^2 \rangle$ in some caging time, provides a local measure of stiffness of the material.[40] Within an idealized model where particles are assumed to be localized by a confining harmonic potential, $\langle u^2 \rangle$ can be thought of as a molecular compliance. While this quantity is only expected to be qualitatively related to the true elastic moduli of the material at temperatures below than T_g, we may expect this quantity to retain some measure of local stiffness at elevated temperatures and to correlate with the dynamic heterogeneity over longer length and time scales.[34] We consider this quantity below for both antiplasticized and pure polymer melts. A particular advantage of $\langle u^2 \rangle$ is that it can be measured experimentally with inelastic neutron or x-ray scattering.

Following previous reports,[16,35] we investigated structural properties using a Voronoi and Delaunay tesselation of space.[41] We focus on the properties of the pure polymer for two reasons. First, the pure polymer exhibited a much higher degree of cooperativity in general, which eases the study of cooperative particle properties. Second, having particles of different sizes introduces some ambiguity into the Voronoi/Delaunay analysis that is unavoidable for the antiplasticized system. From our trajectory files at $T=0.46$, we have isolated 13 configurations that correspond to states just *before* a large degree of cooperativity was observed and constructed the Voronoi volumes and Delaunay simplices for our system. The Voronoi volumes are useful because they characterize the space *around* the particles, while the Delaunay simplices characterize the shape of the space *between* the particles.

Shown in Fig. 5 is the distribution of Voronoi volumes in our system, as well as the volumes for only the mobile particles. There is a clear, albeit small, shift in the average Voronoi volume for mobile particles, indicating that these

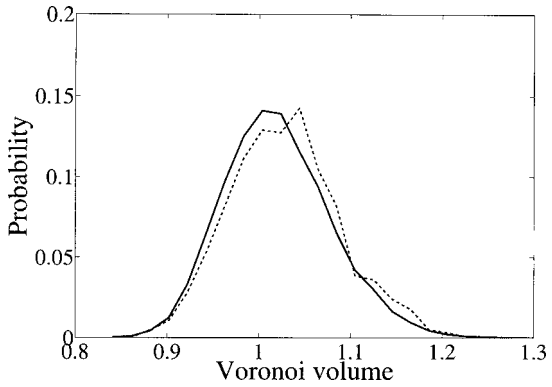

FIG. 5. Probability of finding a monomer with a given Voronoi volume averaged over all particles in the 13 configurations (solid line, see text) and for the mobile particles (dashed line).

particles have slightly more "free volume" surrounding them. However, overall we see from the distributions of Voronoi volumes that the Voronoi volume itself cannot be used as a reliable predictor of particle mobility.[25]

A consideration of the local packing symmetry provides a more reliable indicator of particle mobility; in particular, the tetrahedricity Γ of the Delaunay simplices associated with each atom is a useful measure. Γ is a measure of the deviations of the local environment surrounding a central particle from a perfectly formed tetrahedron; further details on the definition of Γ can be found in Ref. 16. Previous works have shown that this quantity is more indicative of the dynamics than the Voronoi volumes.[16] In Fig. 6, we show the distributions of Γ for all particles in the system and for only the mobile particles. Consistent with a previous work,[16] the environment surrounding the mobile particles is more distorted from a perfect tetrahedral packing. Apparently Γ provides a reasonably good indicator of particle mobility.

We would like to point out that for the pure polymer on the average approximately 70% of the mobile particles are taking part in the cooperative motion (strings) at this temperature, so the behaviors shown here are results for mostly cooperative particles and a small amount of isolated mobile particles. Studying only the cooperative particles has no effect on the distributions shown, however a future work will investigate how these "defects" in the local structure might

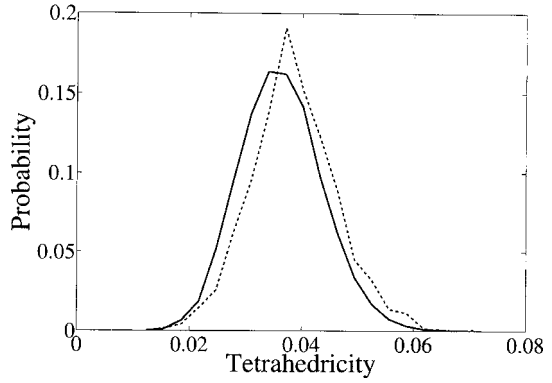

FIG. 6. Probability of finding a monomer with a given tetrahedricity averaged over all particles (solid line) and the mobile particles (dashed line).

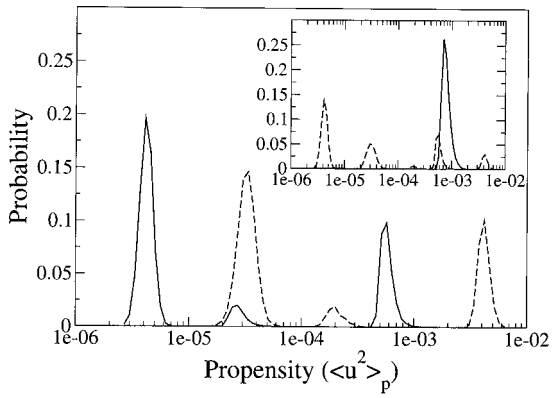

FIG. 7. Main figure: Probability of finding a particle with a given propensity $\langle u^2 \rangle$ for the antiplasticized system. The distribution for the antiplasticized polymer monomers are shown in the solid line and antiplasticizer particles in the dashed line. Inset: Probability distribution of $\langle u^2 \rangle$ for the pure polymer system (solid line) and the antiplasticized system (dashed line).

be connected to each other, as has been shown previously in two-dimensional strongly interacting fluids.[35]

Next, we wish to return to the determination of $\langle u^2 \rangle$. We follow Ref. 34 and use the "isoconfigurational ensemble" in order to calculate $\langle u^2 \rangle$. When calculated in this manner, the Debye-Waller factors are sometimes referred to as the "propensity," which we will denote as $\langle u^2 \rangle_p$. This quantity has the benefit that it does not suffer from any ambiguity due to the different sizes of the two components in the antiplasticized system (as the Vornoi/Delaunay analysis does). Therefore, it can be calculated for both the pure polymer and the antiplasticized polymer. The isoconfigurational ensemble involves averaging from a common time point, and thus enables us to associate values of the propensity with the mobile and immobile particles of a given configuration. We begin with 13 configurations for each system, where each configuration is taken from the longer molecular dynamics runs from above. When we save each configuration, we record which particles are currently defined as mobile (see above) so that the properties of the mobile particles can be analyzed separately from the rest of the system. We then calculate 100 unique MD trajectories for each configuration, each beginning with a different velocity distribution. The mean-square displacement is then calculated during each trajectory at the average collision time t_c for all of the particles in each system. The collision time is defined as the time when the velocity autocorrelation function first becomes negative, and corresponds to a time of $t_c=0.02$ for the pure polymer and $t_c=0.017$ for the antiplasticized polymer, although the results are essentially independent of the choice of t_c. Using the isoconfigurational ensemble prevents the system from ever deviating too far from the starting point, as each trajectory is run for a short total time of $t \approx 100 t_c$.

Figure 7 shows the distribution of the propensity (denoted by $\langle u^2 \rangle_p$) for each system. The difference in the distributions for the pure polymer and the antiplasticized system is quite dramatic. In the inset to Fig. 7, we see that the pure polymer system has a single peak centered around $\langle u^2 \rangle_p = 7.0 \times 10^{-4}$, while the antiplasticized system has *five* unique peaks. We analyze the antiplasticized system in more

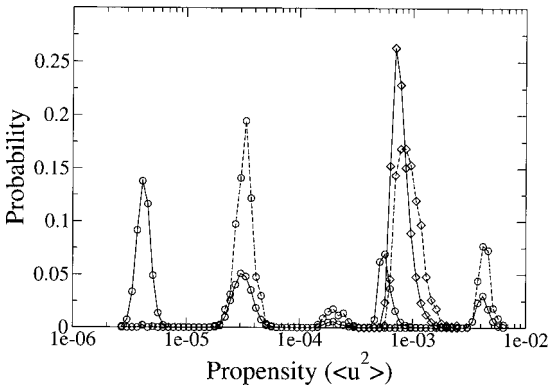

FIG. 8. Change in the propensity distribution with mobility. The distributions for the pure polymer system (◇) and antiplasticized system (○) are shown. The distribution is averaged over all particles in the solid lines, and only the mobile particles in the dashed lines.

detail in the main part of Fig. 7, where the distribution of the propensity is plotted for each component of the antiplasticized system. We find that the polymer monomers exhibit three different values of the propensity, and each one is smaller than that exhibited by the polymer monomers in the pure system. For the antiplasticizer particles, we also find three distinct peaks. Interestingly, we find that each peak is unique to one of the species, except for the peak centered around $\langle u^2\rangle_p = 3.0 \times 10^{-5}$. This peak has a contribution from both the polymer monomers and the antiplasticizer particles.

In Fig. 8 we see how the distribution of $\langle u^2\rangle_p$ changes if we only look at the mobile particles. First, for the pure polymer system, we see that the distribution of $\langle u^2\rangle_p$ amongst the mobile particles is slightly higher, consistent with previous works.[34] For the antiplasticized system, the behavior is once again more complex than in the pure polymer. We find that none of the mobile particles have a peak propensity associated with the smallest value of $\langle u^2\rangle$. Interestingly, there are also no mobile particles associated with the peak associated with the second-highest value of the propensity at $\langle u^2\rangle = 5.0 \times 10^{-4}$. Each of the other peaks correspond to a substantial amount of mobile particles, and each peak is shifted slightly to higher values of $\langle u^2\rangle$, though the shift is not as prominent as it is in the pure polymer system.

Now that we have confirmed the previous finding that $\langle u^2\rangle_p$ can be a reliable indicator of long-time mobility[34] it is of our interest to show the spatial distribution of $\langle u^2\rangle_p$ for each system. We show in Fig. 9 a color map of $\langle u^2\rangle_p$ for a typical configuration at a common reduced temperature for each system ($T/T_c = 1.1$), where local values of $\langle u^2\rangle$ are determined by averaging over cubes with sides of length $l \approx 1.95\sigma_A$. While antiplasticization leads to an improvement in the packing efficiency, as evidenced by a higher density and stronger glass formation,[11] these maps show that $\langle u^2\rangle_p$ exhibits an opposite tendency. In particular, $\langle u^2\rangle_p$ exhibits large fluctuations over small length scales in the antiplasticized system. The amplitude of the fluctuations in the pure polymer is much smaller (note the difference in scale on each colormap). These findings indicate that, in terms of the propensity, the pure polymer is more homogeneous in terms of the propensity. One interpretation of Debye-Waller factors,

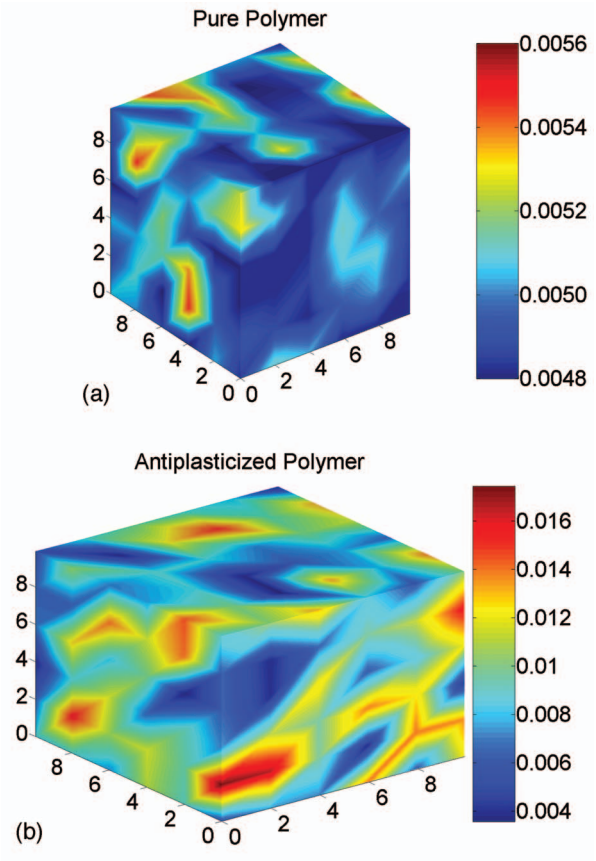

FIG. 9. (Color) Local propensities in the pure polymer (top) and the antiplasticized system (bottom). Length scales are in units of σ_A, and the propensity values are averaged over local cubes with sides of length $l \approx 1.95\sigma_A$. Note that the scale is different on each color bar, with the range larger on the antiplasticized case.

or $\langle u^2\rangle_p$, is that they provide a measure of the local stiffness of the material,[40] where $k_B T/\langle u^2\rangle$ is an elastic constant defining the localization of the particles on time scales between the ballistic regime and the structural relaxation. Of course, this simple interpretation is based on treating the particles as being harmonically confined within an idealized elastic matrix, but we still believe that $\langle u^2\rangle_p$ provides a measure of local stiffness in a qualitative sense. If one adopts this view, these local fluctuations of $\langle u^2\rangle$ could have important consequences in the interpretation of the boson peak, which remains largely unexplained.[42,43] Several recent studies have provided compelling arguments that the position and intensity of the boson peak can be understood in terms of the length scale and magnitude of the fluctuations in the elastic constants.[44–49]

VI. CONCLUSIONS

In conclusion, we have shown that the model proposed here exhibits many of the canonical features of antiplasticized polymer melts. The addition of small-molecule diluents to a coarse-grained polymer melt antiplasticizes the system by enhancing the shear modulus (G'), increasing the density below the pure T_g and by reducing T_g. The tendency of the system to move via a stringlike motion is diminished considerably in the antiplasticized melt, which exhibits much

smaller-scale collective motions. Additionally, the lengths of the strings for the pure polymer grow longer as the temperature decreases, while for the antiplasticized system the temperature dependence of the string lengths is relatively weak. This behavior correlates well with the fragility of the system and the expected behaviors from the Adam-Gibbs description of relaxation in glass-forming liquids,[12,14] where the strings are identified with the cooperatively rearranging regions of the Adam and Gibbs model. Antiplasticization has the effect of making the glass a stronger glass former in the model systems studied here. Unexpectedly, it is found that the stringlike collective motion becomes increasingly concentrated in antiplasticizer molecules upon cooling. The generality of the latter observation should be addressed in future works. Finally, we have investigated structural indications of mobility, and we found that the tetrahedricity of the Delaunay simplices correlates very well with mobility in our pure polymer system, as does the short-time values of the local mean-squared displacement $\langle u^2 \rangle_p$, which has been termed the "propensity."[34] The behaviors of the propensity in multicomponent systems will be the subject of future investigations.

We expect this understanding of antiplasticization to have important applications in the preservation of biological materials[50] and in the mechanical stability of nanoscale polymer structures employed in the semiconductor industry.[51] Recently, we have shown how reducing the length of cooperative regions (strings) through antiplasticization leads to a drastic reduction of confinement effects in thin (unsupported) polymer films.[28] It has also been shown that confinement leads to a reduction in the fragility of polymers.[13,52] Taken with the results presented in this paper, we propose that confinement effects will be less pronounced in stronger glass-forming materials than in fragile glass-forming systems. Since confinement tends to reduce fragility, a material that already exhibits a reduced fragility, such as an antiplasticized polymer, may be less susceptible to changes of its physical properties (such as T_g) upon confinement. This picture is consistent with our previous results[28] and the experimental results of Ref. 53, where it was shown that a small amount of pyrene can eliminate the effects of confinement in poly(styrene).

ACKNOWLEDGMENTS

This work was supported by the SRC (No. 2005–06–985) and the NSF (NIRT Grant No. CTS-0506840).

[1] J. M. G. Cowie, *Polymers: Chemistry and Physics of Modern Materials*, 2nd ed. (Nelson, Cheltenham, 1998).
[2] J. Ferry, *Viscoelastic Properties of Polymers* (Wiley, New York, 1980).
[3] Y. Maeda and D. Paul, J. Polym. Sci., Part B: Polym. Phys. **25**, 957 (1987).
[4] R. Casalini, K. Ngai, C. Robertson, and C. Roland, J. Polym. Sci., Part B: Polym. Phys. **38**, 1841 (2000).
[5] P. Ghersa, Mod. Plast. **36**, 135 (1958).
[6] Y. Maeda and D. Paul, J. Polym. Sci., Part B: Polym. Phys. **25**, 1005 (1987).
[7] K. L. Ngai, R. W. Rendell, A. F. Yee, and D. J. Plazek, Macromolecules **24**, 61 (1991).
[8] A. K. Rizos, L. Petihakis, K. L. Ngai, J. Wu, and A. F. Yee, Macromolecules **32**, 7921 (1999).
[9] J. Vrentas, J. Duda, and H. Ling, Macromolecules **21**, 1470 (1988).
[10] B. J. Cauley, C. Cipriani, K. Ellis, A. K. Roy, A. A. Jones, P. T. Inglefield, B. J. McKinley, and R. P. Kambour, Macromolecules **24**, 403 (1991).
[11] J. Dudowicz, K. F. Freed, and J. F. Douglas, J. Phys. Chem. B **109**, 21350 (2005).
[12] G. Adam and J. Gibbs, J. Chem. Phys. **43**, 139 (1965).
[13] T. S. Jain and J. J. de Pablo, J. Chem. Phys. **120**, 9371 (2004).
[14] J. Dudowicz, K. F. Freed, and J. F. Douglas, J. Chem. Phys. **123**, 111102 (2005).
[15] C. Donati, J. F. Douglas, W. Kob, S. J. Plimpton, P. H. Poole, and S. C. Glotzer, Phys. Rev. Lett. **80**, 2338 (1998).
[16] T. S. Jain and J. J. de Pablo, J. Chem. Phys. **122**, 174515 (2005).
[17] K. Yoshimoto, T. S. Jain, P. F. Nealey, and J. J. de Pablo, J. Chem. Phys. **122**, 144712 (2005).
[18] K. Yoshimoto, T. Jain, K. V. Workum, P. F. Nealey, and J. J. de Pablo, Phys. Rev. Lett. **93**, 175501 (2004).
[19] C. Bennemann, W. Paul, J. Baschnagel, and K. Binder, J. Phys.: Condens. Matter **11**, 2179 (1999).
[20] S. Sastry, P. Debenedetti, and F. Stillinger, Nature (London) **393**, 554 (1998).
[21] M. D. Ediger, C. A. Angell, and S. R. Nagel, J. Chem. Phys. **100**, 13200 (1996).
[22] C. A. Angell, J. Phys. Chem. Solids **49**, 863 (1988).
[23] A. R. C. Baljon, M. H. M. Van Weert, R. B. DeGraaf, and R. Khare, Macromolecules **38**, 2391 (2005).
[24] F. Varnik, J. Baschnagel, and K. Binder, Phys. Rev. E **65**, 021507 (2002).
[25] F. W. Starr, S. Sastry, J. F. Douglas, and S. C. Glotzer, Phys. Rev. Lett. **89**, 125501 (2002).
[26] *Computer Simulation of Liquids*, edited by M. P. Allen and D. J. Tildeslay (Clarendon, Oxford, 1987).
[27] P. G. Debenedetti and F. H. Stillinger, Nature (London) **410**, 259 (2001).
[28] R. A. Riggleman, K. Yoshimoto, J. F. Douglas, and J. J. de Pablo, Phys. Rev. Lett. **97**, 045502 (2006).
[29] M. Aichele, Y. Gebremichael, F. W. Starr, J. Baschnagel, and S. C. Glotzer, J. Chem. Phys. **119**, 5290 (2003).
[30] M. N. J. Bergroth, M. Vogel, and S. C. Glotzer, J. Phys. Chem. B **109**, 6748 (2005).
[31] V. Teboul, A. Monteil, L. Fai, A. Kerrache, and S. Maabou, Eur. Phys. J. B **40**, 49 (2004).
[32] J. F. Douglas, J. Dudowicz, and K. F. Freed, J. Chem. Phys. **125**, 144907 (2006).
[33] V. Teboul, A. Monteil, L. Fai, A. Kerrache, and S. Maabou, Eur. Phys. J. B **40**, 49 (2004).
[34] A. Widmer-Cooper and P. Harrowell, Phys. Rev. Lett. **96**, 185701 (2006).
[35] C. Reichhardt and C. J. O. Reichhardt, Phys. Rev. Lett. **95**, 095504 (2003).
[36] U. Buchenau and R. Zorn, Europhys. Lett. **18**, 523 (1992).
[37] A. P. Sokolov, E. Rössler, A. Kisliuk, and D. Quitmann, Phys. Rev. Lett. **71**, 2062 (1993).
[38] J. F. Lutsko, J. Appl. Phys. **64**, 1152 (1998).
[39] M. D. Kluge, D. Wold, J. F. Lutsko, and S. R. Phillpot, J. Appl. Phys. **67**, 2370 (1989).
[40] G. Zaccai, Science **288**, 1604 (2000).
[41] D. C. Rapaport, *The Art of Molecular Dynamics Simulation* (Cambridge University Press, Cambridge, 2004).
[42] C. A. Angell, Y. Yue, L.-M. Wang, J. R. D. Copley, S. Borick, and S. Mossa, J. Phys.: Condens. Matter **15**, S1051 (2003).
[43] C. A. Angell, J. Phys.: Condens. Matter **16**, S5153 (2004).
[44] A. P. Sokolov, R. Calemczuk, B. Salce, A. Kisliuk, D. Quitmann, and E. Duval, Phys. Rev. Lett. **78**, 2405 (1997).
[45] F. Léonforte, A. Tanguy, J. P. Wittmer, and J. L. Barrat, Phys. Rev. Lett. **97**, 055501 (2006).
[46] F. Léonforte, R. Boissiere, A. Tanguy, J. P. Wittmer, and J.-L. Barrat, Phys. Rev. B **72**, 224206 (2005).
[47] B. Rossi, G. Viliani, E. Duval, L. Angelani, and W. Garber, Europhys. Lett. **71**, 256 (2005).
[48] W. Schirmacher, Europhys. Lett. **73**, 892 (2006).
[49] V. N. Novikov, Y. Ding, and A. P. Sokolov, Phys. Rev. E **71**, 061501 (2005).

[50] G. Caliskan, D. Mechtani, J. H. Roh, A. Kisliuk, A. P. Sokolov, S. Azzam, M. Cicerone, S. Lin-Gibson, and I. Peral, J. Chem. Phys. **121**, 1978 (2004).
[51] M. P. Stoykovich, H. B. Cao, K. Yoshimoto, L. E. Ocola, and P. F. Nealey, Adv. Mater. (Weinheim, Ger.) **14**, 1180 (2003).
[52] K. Fukao and Y. Miyamoto, Phys. Rev. E **64**, 011803 (2001).
[53] C. J. Ellison, R. L. Ruszkowski, N. J. Fredin, and J. M. Torkelson, Phys. Rev. Lett. **92**, 095702 (2004).